Heliyon 6 (2020) e04137

Contents lists available at ScienceDirect

Heliyon

journal homepage: www.cell.com/heliyon

Research article

Sensing the classical swine fever virus with molecularly imprinted polymer on quartz crystal microbalance

Supaporn Klangprapan [a], Benjarat Choke-arpornchai [b], Peter A. Lieberzeit [c,*], Kiattawee Choowongkomon [d,e,**]

[a] Genetic Engineering Interdisciplinary Program, Graduate School, Kasetsart University, 50 Ngam Wong Wan Road, Chatuchak, Bangkok, 10900, Thailand
[b] Department of Chemistry, Faculty of Science, Chulalongkorn University, 254 Phyathai Road, Patumwan, Bangkok, 10330, Thailand
[c] University of Vienna, Faculty for Chemistry, Department of Physical Chemistry, Waehringer Strasse 42 A-1090 Wien, Austria
[d] Department of Biochemistry, Faculty of Science, Kasetsart University, 50 Ngam Wong Wan Road, Chatuchak, Bangkok, 10900, Thailand
[e] Center for Advanced Studies in Nanotechnology for Chemical, Food and Agricultural Industries, KU Institute for Advanced Studies, Kasetsart University, Bangkok, Thailand

ARTICLE INFO

Keywords:
Analytical chemistry
Classical swine fever virus
Molecular imprinting
Quartz crystal microbalance

ABSTRACT

Classical swine fever (CSF) is a highly contagious and fatal viral disease in pigs caused by the virus of the same name (classical swine fever virus – CSFV). Economical reasons dictate the need for rapid early detection of this pathogen. Herein we report on a sensor for CSFV detection based on a quartz crystal microbalance (QCM) making use of molecularly imprinted polymer (MIP) as the receptor. It relies on a copolymer comprising acrylamide (AAM), methacrylic acid (MAA), methyl methacrylate (MMA), and n-vinylpyrrolidone (VP). SEM images of CSFV MIP reveal cavities on the polymer surface with an average diameter of d = 59 nm, which correlates well with the dimensions of CSFV particles. QCM sensor measurements yield concentration-dependent CSFV sensor responses resulting in LOD = 1.7 μg/mL, LOQ = 5.1 μg/mL and R^2 = 0.9963. Furthermore, CSFV-MIP sensors selectively bind CSFV with selectivity factors of 2 over porcine respiratory and reproductive virus (PRRSV) and 62 over pseudorabies virus (PRV), respectively. Finally, sensor responses turned out fully reversible.

1. Introduction

Classical swine fever (CSF), also known as hog cholera, is a highly contagious and fatal viral disease in pigs caused by the classical swine fever virus (CSFV). The World Organization for Animal Health (OIE) classifies CSF as a specific hazard of importance in international trade (OIE, 2020). Any outbreak has to be reported, because it can severely affect pork exports from the whole country affected. It has been causing serious problems in pig industry in various parts of the world (Mukherjee et al., 2018; Postel et al., 2018). CSFV is a member of the genus *Pestivirus* within the family *Flaviviridae* (Shi et al., 2009) (Beer et al., 2015). The CSFV virion is an icosahedral particle. The electron density is very high in the inner core structure of about 30 nm. This is surrounded by a globular envelope with diameters ranging between 40 and 60 nm (Moennig, 2000) (Moennig et al., 2003). CSFV spreads by contacts among live pigs, or by feeding pigs with contaminated pig meat. Once the virus breaks out, it severely diminishes pork exports from the region concerned and thus leads to substantial financial loss. Vaccination is one of the measures to control CSF. However, this leads to problems, when aiming to detect CSFV by indirect enzyme-linked immunosorbent assay (ELISA): this method cannot distinguish between pigs that have been vaccinated and those infected with wild type CSFV, because the animals of course produce antibodies against CSFV after vaccination. Therefore, both infected and vaccinated animals will yield positive ELISA results. Furthermore, ELISA tests may cross-react with other pestiviruses, such as border disease virus (BDV), and bovine viral diarrhea virus (BVDV) (Panyasing et al., 2018) (Postel et al., 2015). Finally, ELISA tests require following somewhat complex protocols.

Given the high economic impact, there is an extensive body of research on analyzing CSFV. Detection strategies include a variety of methods, such as loop mediated isothermal amplification (LAMP) (Postel et al., 2015), flow cytometry (Hua et al., 2014), and reverse transcriptase polymerase chain reaction (RT-PCR) analysis (Petrini et al., 2017). However, such methods are often time-consuming and come with high

* Corresponding author.
** Corresponding author.
E-mail addresses: Peter.Lieberzeit@univie.ac.at (P.A. Lieberzeit), kiattawee.c@ku.th (K. Choowongkomon).

https://doi.org/10.1016/j.heliyon.2020.e04137
Received 13 March 2020; Received in revised form 25 May 2020; Accepted 1 June 2020

instrument and maintenance costs. Moreover, there are also reports on sensing CSFV utilizing e.g. Surface Plasmon Resonance (SPR) investigating the interaction between CSFV and serum antibody on sensor chip surfaces in relative time (Mustafa et al., 2014). Another approach utilizes anti-CSFV IgG deposited on magnetoelastic (ME) sensors. The recognition reaction leads to mass changes and hence significant change in resonance frequency of the biosensor (Guo et al., 2016). Furthermore, Lu et al. introduced a colorimetric split G-quadruplex DNAzyme to sense CSFV RNA (Lu et al., 2017).

All those sensors rely either on amplifying genetic material of CFSV, or on recognition systems that originate from nature. However, when aiming at bringing sensors to markets, such natural systems are not optimal regarding their limited ruggedness and the possibility to upscale production processes. Addressing those points, molecularly imprinted polymers (MIPs) (Piletsky et al., 2017; Xu et al., 2017) are the result of template-directed synthesis that leads to structures with excellent recognition of the respective target species. This comprises both their shape and functionality on the surface. MIP are usually inexpensive and yield high affinity and selectivity reaching those of natural receptors. They combine stability and straightforward preparation. This makes them interesting for sensing biological species (Kupai et al., 2017) among other analytes. Quartz Crystal Microbalance (QCM) is a transducer that measures small mass changes on the sensor surface. Coating it with MIPs has led to powerful sensors (Croux et al., 2012). Especially surface imprinting is of interest, because it creates binding cavities of the target directly on the surface of a cross-linked polymer layer, which makes it comparably easy to remove the template (Eersels et al., 2016). There is a variety of literature on MIP-based QCM sensors for biospecies demonstrating their feasibility in principle: Recent examples include sensors towards bovine serum albumin (Phan et al., 2018), a sensor based on the dopaminergic receptor (Naklua et al., 2016), toward *Escherichia coli* (Poller et al., 2017), influenza A virus (Wangchareansak et al., 2013), and Dengue virus (Lieberzeit et al., 2016). In the light of previous work, we herein report on designing MIP-QCM sensors to detect CSFV (see Figure 1). This is also interesting among others, because it draws the focus on animal pathogens rather than human diagnostics, which potentially opens up new application scenarios. One can expect such systems to be good-value: the reagents needed for manufacturing MIP are usually bulk chemicals. Quartz blanks come at a cost of roughly 1€/substrate. Therefore, it is realistic to assume that one sensor costs well below 10€. Read-out systems are feasible at costs of a few hundred to a few thousand Euros (or a bit higher), depending on the needs of the customer and manufacturing numbers.

2. Materials & methods

2.1. Chemicals and materials

The monomers acrylamide (AAM), methacrylic acid (MAA), methyl methacrylate (MMA) and N-vinylpyrrolidone (VP), the cross-linker dihydroxyethylene-bisacrylamide (DHEBA), the initiator 2, 2′-azobis (isobutyronitrile) (AIBN), and dimethyl sulfoxide (DMSO) were purchased form Sigma-Aldrich and VWR, respectively, in highest available purity for synthesis or analytical purity. To prepare MIP, we utilized classical swine fever (Hog cholera) live vaccine from Green Cross Veterinary Products Co., Ltd., Korea, as the template CSFV: in contrast to wild types, these are non-pathogenic and can be handled more easily. Porcine reproductive and respiratory syndrome virus (PRRSV) and pseudorabies virus (PRV) were isolated from cell culture-derived PRRSV and PRV provided from BF feeds company, Thailand. 0.1 M PBS buffer pH 7.4 served for preparing the PRRSV and PRV samples. All virus preparations required laboratories on biosafety level 1. For frequency measurements, we utilized a network analyzer (Agilent Technologies E5062A ENA series), laboratory power supplies (EA-PS 2032-025), and a frequency counter (Agilent Technologies 53131A).

2.2. Preparation of virus

All experiments relied on CSFV from vaccine: this contains live attenuated virus at a concentration of 10^3 medium Tissue culture Infectious Dose estimation ($TClD_{50}$/mL) converted to μg/mL by using nanodrop spectrophotometer at $\lambda = 280$ nm. For preparing MIP, we used the CSFV vaccine as received, i.e. without any workup/pretreatment. PRRSV and PRV for selectivity tests were isolated from cell culture: Briefly, for that purpose we froze infected cell culture medium to -20 °C followed by thawing at room temperature, and repeated this cycle for 3 times. Afterwards, we centrifuged at 5000g and 4 °C for 30 min. After collecting the supernatant and discarding the pellet, we added dimethicone (PEG 8000) to the supernatant until reaching a final PEG concentration of 10 %, stirred gently at 4 °C, overnight, centrifuged at 10800g and 4 °C for 30 min, collected the pellet, and re-suspended it in TNE buffer. Then we separated the virus from other components in the pellet by using sucrose gradient 10–60% in an ultracentrifuge tube and overlaying it with the pellet solution. During centrifugation, a white ring formed in the tube, which contains the virus. We collected that phase by the means of an injection needle followed by washing the pellet by adding PBS buffer pH 7.4 and centrifugation at 10,800 g and 4 °C for 60 min. Virus stock solutions comprised of these pellets re-suspended in PBS buffer and stored at -20 °C until use. Scanning electron microscopy (SEM) served to characterize the viruses and to confirm their size and shape before sensor experiments. All these experiments took place in a strictly controlled laboratory (biosafety level 1).

2.3. Preparing quartz crystal microbalances

For depositing Au electrodes on 10 MHz AT-cut quartz plates with 13.8 mm in diameter (purchased from Roditi Inc., United Kingdom), we used a previously published procedure (Chunta et al., 2016). Briefly, the process comprised of screen-printing the respective dual–electrode structures with 5 mm diameter and 19.62 mm^2 area each using brilliant gold paste and burning them at 400 °C for 4 h to remove organic components and reveal the blank gold electrodes. After electrode deposition, we characterized all QCM sensors by recording their respective damping spectra around the resonance frequency with a network analyzer (Agilent Technologies E5062A ENA series).

2.4. Polymer synthesis

For synthesizing MIP, we relied on a previously published polymer system that proved highly suitable for sensing influenza virus particles (Wangchareansak et al., 2013). Briefly, the mixture contained four different monomers, AAM (13 mg; 101.6 μmol), MAA (10.6 μl; 65.8 μmol), MMA (6 μl; 31.2 μmol), VP (6.3 μl; 31.2 μmol). To this, we added DHEBA (47 mg; 130.4 μmol) as a crosslinking agent and 300 μl of dimethyl sulfoxide (DMSO) in a 1.5 mL Eppendorf tube and mixed well. Finally, we added AIBN (1 mg; 3.4 μmol) as an initiator followed by ultrasonication for 1 min to remove dissolved gasses and then stirring at 70 °C for approximately 30 min until just prior to reaching the gel point. These pre-polymers remained refrigerated at 4 °C for CSFV imprinting.

2.5. Preparing MIP-QCM sensors

Before imprinting, it was necessary to clean QCM electrodes with 70% aqueous ethanol solution followed by drying at room temperature. Then, we spin-coated 2 μl of pre-polymer solution on the two electrodes each at 1000 rpm for 35 s to obtain flat oligomer thin films. In parallel, we drop-coated 5 μl CSFV solution from vaccine onto a glass slide roughly 0.5 cm × 0.5 cm in size and incubated for 2 h in a refrigerator before stamping it onto the oligomer thin film on the working side of the QCM. Leaving the prepared devices under UV light ($\lambda = 312$ nm) overnight and washing the template with 10% v/v of (acetic acid for 3 h followed by distilled water for 1 h) led to the final devices. The reference side containing the NIP was prepared in the same way except for

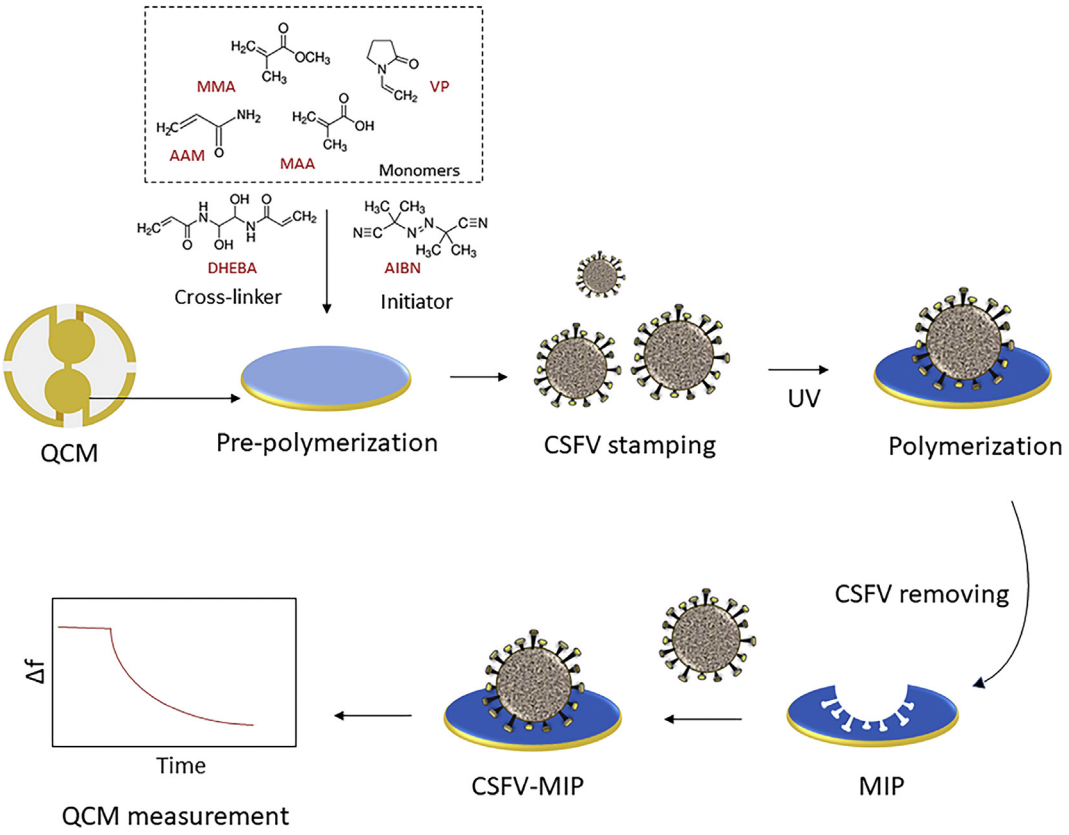

Figure 1. Schematic representation of preparing MIP-QCM sensors.

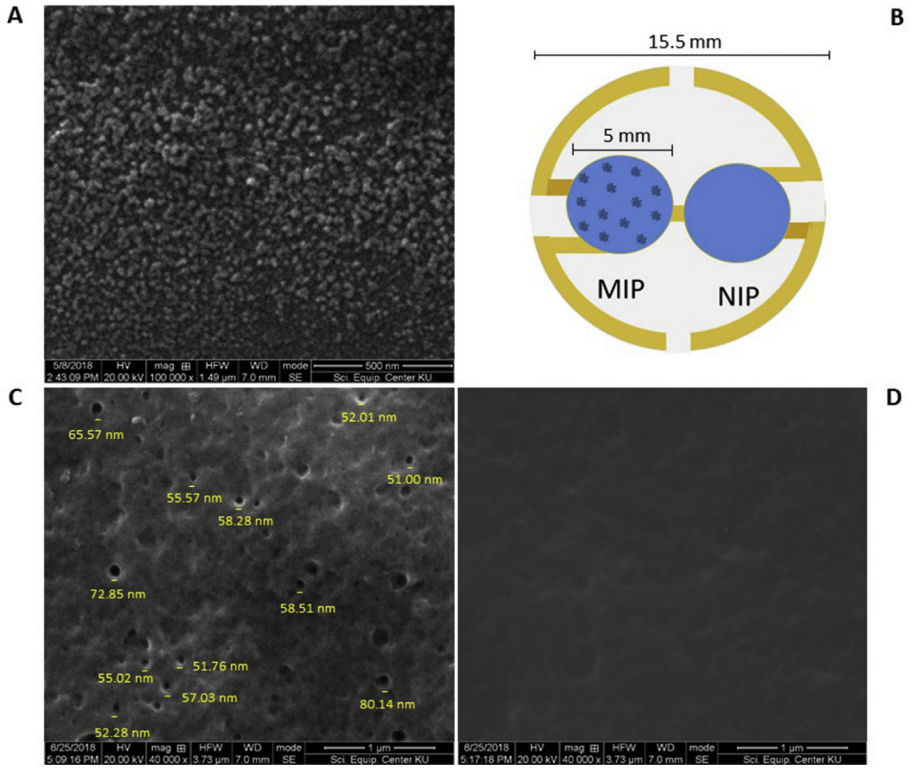

Figure 2. SEM images of (A) CSFV particles from CSFV vaccine with particles were size between 30-60 nm. (B) MIP and NIP side on gold surface. (C) CSFV imprinted on polymer (MIP) surface show small cavities (roughly 2.22 cavities/μm^2) with average sizes 59 nm. (D) Non-imprinted polymer (NIP), i.e. blank co-polymer surface.

leaving out the template (see Figure 2B). This allows for compensating any frequency effects of fluctuating temperature, liquid density, or viscosity, because these effects contribute equally to the signals on both channels. The approach resulted in layers roughly 100–200 nm thick. Furthermore, we characterized MIP and NIP surfaces by scanning electron microscopy.

2.6. Sensor measurements

For sensor measurements, we connected the QCM to a custom-made dual oscillator for active measurements. A Frequency counter (Agilent Technologies 53131A) read out the frequencies of the two channels as a function of time. A homemade software transferred this data to a PC. Before exposing sensors to samples, we left them to equilibrate in water or the background buffer, until they reached stable baseline at room temperature. Then we carried out the following sequence of steps: First, we loaded 100 µl of CSFV suspension into the measuring cell, so that the virus could attach to the respective polymer layers. During this step, we recorded the corresponding change in frequency signal. After the signal reached stable value, we paused the read-out software and washed the cell by loading it repeatedly with DI water and removing it again for 10 times or more. Then, we re-started the software to observe the signal return to the base line position. During sensitivity measurements, we repeated these steps using suspensions containing different amounts of the virus. In the case of selectivity testing, we used PRRSV and PRV instead and compared their responses to those of CSFV. All measurements took place in triplicate.

2.7. Characterization of CSFV and MIP

We recorded all SEM images on a Quanta 450 FEI scanning electron microscope. Secondary electrons were generated at 25 keV and EDS (Energy Dispersive X-ray Spectroscopy). CSFV samples were dropped on the glass slide and dehydrated with ethanol series by subsequent exchanges of dilutions in distilled water (25, 50, 75, 100 % EtOH). Then, the virus was dried with critical point drying (CRD) to protect its surface structures from shrinking and collapsing. CSFV and polymers, respectively, were coated with carbon to obtain conductive surfaces before scanning.

3. Results and discussion

3.1. CSFV-MIP surface characterization

In a first step, it was necessary to confirm that the MIP surface contains actual virus imprints. Figure 2A shows SEM images of a CSFV stamp surface: It clearly reveals globular structures with 30–60 nm diameter at 100000 times magnification, which corresponds well to the known size of CSFV (Moennig, 2000). For instance, Wang et al., (2015) reported that CSFV particles purified from cell culture by ultrafiltration are around 50 nm in diameter. In addition, one can see both separate and aggregated CSFV particles on the glass surface, respectively. Figure 2C shows a MIP layer after removing CSFV particles. It reveals surface cavities with an average diameter of d = 59 nm. The image allows for estimating cavity density equal to roughly 2 cavities/µm^2. This leads to an estimate of 4.4 $\times$ 10^4 cavities per MIP electrode. However, these figures only estimate the order of magnitude: actually "calibrating" those surfaces would require calculating the average results of a large number of SEM images, which is beyond the scope of this article. In contrast to this, the NIP surface does not reveal any cavities (see Figure 2D). Therefore, SEM analysis clearly demonstrates successful structuring of the MIP surfaces.

3.2. MIP sensor responses

However, generating cavities that correspond to the diameter of CSFV *per se* is not sufficient. The cavities also need to incorporate the virus and bind it selectively to make them useful for sensing. Figure 3A shows the QCM sensor responses both of MIP and NIP, respectively, when exposed to different concentrations of CSFV. First, the frequency shifts obtained for MIP are higher than those for NIP at all CSFV concentrations: for instance, at c = 21 µg/mL CSFV, the frequency response of the MIP channel is six times larger, than the corresponding reference signal of the NIP, thus demonstrating an imprinting factor of the same size. As in previous MIP for viruses, one can expect that such binding being the result of both adapted cavity size and template-directed generation of a non-covalent binding network in the polymer. The latter comprises functional groups that optimally interact with the outer shell of the template species. The MIP QCM sensors show frequency signals down to c = 4 µg/mL CSFV, but not below this concentration (Figure 3A). Furthermore, all frequency responses are fully reversible after washing the sensors with distilled water. Figure 3B sketches the sensor characteristics resulting from this MIP-QCM sensor. It reveals linear relationship in the concentration range 4–21 µg/mL CSFV. It does not make sense to test higher levels: first, the upper detection limit of a sensor is not important for rapid screening of possible infection in pigs. Second, all measurements rely on vaccine, which thus represents the highest CSFV concentration available for this study. Limit of detection (LOD) and limit of quantitation (LOQ) of MIP sensor based on QCM measurement were calculated from the equation in Figure 3B, that plots the frequency shifts against the corresponding concentrations between 4 - 21 µg/mL with R^2 = 0.9963. Calculation reveals LOD = 1.7 µg/mL with responses of resonance frequency about 38 Hz/µg/mL. The respective LOQ is 5.1 µg/mL, respectively. Therefore, the LOD we reached is slightly higher than in a study that measured CSFV by using anti-CSFV IgG immobilized on a magnetoelastic sensor (ME): that work reveals sensitivity of about 95 Hz/µg/mL, with a detection limit of 0.6 µg/mL (Guo et al., 2016). It also relies on artificial recognition and straightforward transducers. This clearly demonstrates that such biomimetic approaches indeed can reach the response characteristics of natural receptors such as IgG.

3.3. Selectivity and reproducibility

In addition to sensitivity, selectivity of CSFV-MIP and the control NIP is also a key parameter for characterizing the sensors. We therefore

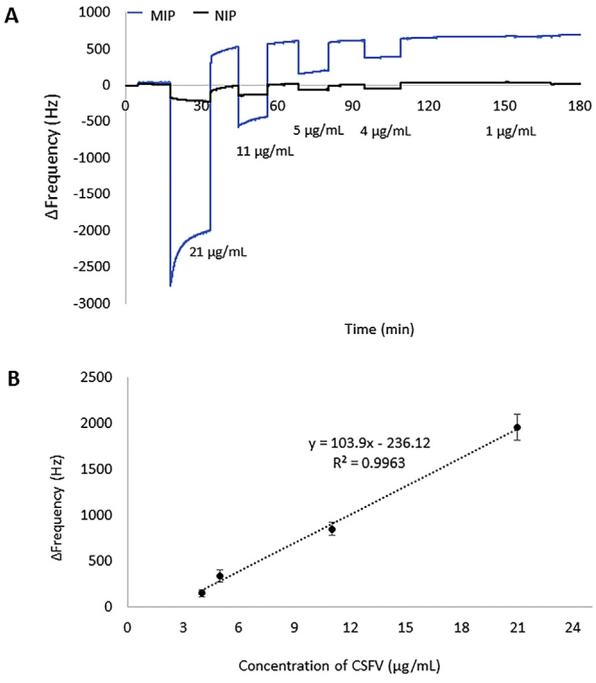

Figure 3. (A) Sensor responses of MIP to difference concentration of CSFV. (B) Sensor characteristic of Figure 3A based on the difference in frequency shifts between MIP and NIP (R^2 = 0.9963).

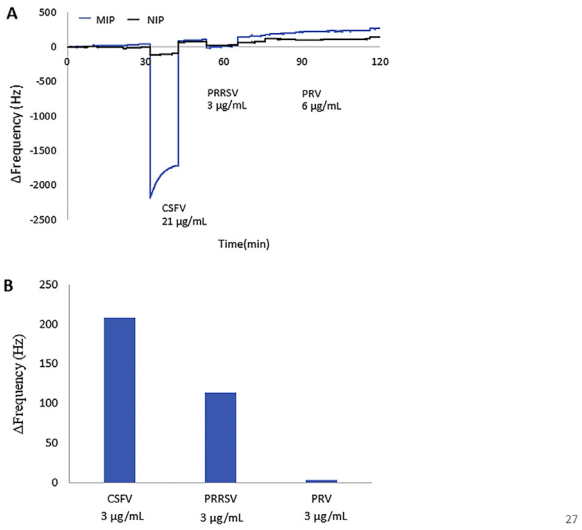

Figure 4. Sensor responses of MIP and NIP (A) to select with difference of virus; 21 μg/mL of CSFV, 3 μg/mL of PRRSV and 6 μg/mL of PRV. (B) Response pattern of MIP-QCM sensor towards CSFV, PRRSV, and PRV.

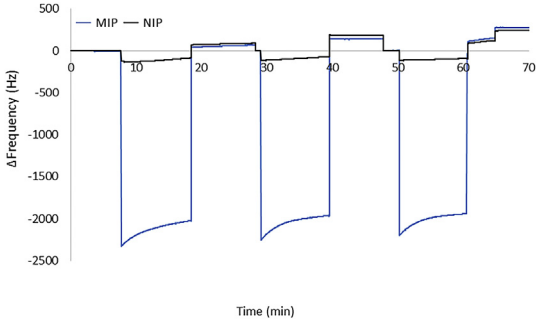

Figure 5. Reproducibility of MIP sensor repeatedly tested for 3 times of 21 μg/mL of CSFV samples.

compared the sensor responses towards three types of virus, namely CSFV, PRRSV, and PRV. Figure 4 shows the results: it reveals that the frequency responses to CSFV (21 μg/mL) are substantially larger than those PRRSV (3 μg/mL) and PRV (6 μg/mL), respectively. Normalizing those responses to the same concentration – 3 μg/mL – leads to the data shown in Figure 4B. It clearly demonstrates that CSFV-MIP sensors bind CSFV with selectivity factors of 2 over PRRSV and 62 over PRV. Obviously, not only particle diameters determine selectivity: the average PRRSV particle diameter is d = 70 nm (Uribe-Campero et al., 2015), which is somewhat larger than that of CSFV (d = 50–60 nm) (Moennig, 2000). Given the size distribution, one can expect that some PRRSV virions fit into cavities on the CSFV-MIP, which leads to minor frequency responses to PRRSV. Furthermore, it is a bit more affine to the polymer, as shown by the frequency shifts of the NIP-coated electrode. This slightly higher inherent affinity of PRRSV makes the selectivity of the MIP even more remarkable. In contrast, PRV are about d = 200–250 nm in diameter (Pomeranz et al., 2005), which of course makes them substantially larger than CSFV-MIP cavities. Overall, the MIPs hence lead to very appreciable selectivity between these three pig pathogens.

Finally, Figure 5 summarizes reproducibility of the sensor responses: exposing a CSFV MIP sensor repeatedly to suspensions containing 21 μg/mL CSFV reveals almost constant sensor responses, namely -2127, -2046, and -2011 Hz, respectively. Furthermore, sensor signals turned out fully reversible: any bound virion particles detached from the MIP surfaces when flushing the system with distilled water.

4. Conclusion

The huge flexibility of MIP synthesis allows for designing recognition systems towards pathogens in comparably short time to make them accessible for rapid analysis. In that sense the MIP/QCM sensor demonstrated herein opens up one way for rapid testing of CSFV, an animal pathogen. Of course, it represents first proof of concept rather than a final product. It is of interest, however, that in this case one can use the vaccine for preparing the MIP in this case. In a next step it will be necessary to test the sensors against the wild type of the virus. However, this is beyond the scope of this paper, not least because handling infective wildtype pathogens requires strict biosafety laboratories that are not available at the authors' institutions.

Declarations

Author contribution statement

Peter Lieberzeit, Kiattawee Choowongkomon: Conceived and designed the experiments; Analyzed and interpreted the data; Contributed reagents, materials, analysis tools or data; Wrote the paper.

Supaporn Klangprapan: Conceived and designed the experiments; Performed the experiments; Analyzed and interpreted the data.

Benjarat Choke-arpornchai: Performed the experiments; Analyzed and interpreted the data.

Funding statement

Supaporn Klangprapan was supported by Thailand Research Fund (PHD60I0086).

Competing interest statement

The authors declare no conflict of interest.

Additional information

No additional information is available for this paper.

Acknowledgements

The authors warmly thank Dr. Tawatchai Hoonsuwan, BF feeds Co. Ltd., Thailand for kindly provided CFSV vaccine, PRRSV and PRV infected cell culture media.

References

Beer, M., Goller, K.V., Staubach, C., Blome, S., 2015. 'Genetic variability and distribution of Classical swine fever virus. Anim. Health Res. Rev. 16, 33–39.

Chunta, S., Suedee, R., Lieberzeit, P.A., 2016. 'Low-Density lipoprotein sensor based on molecularly imprinted polymer. Anal. Chem. 88, 1419–1425.

Croux, D., Weustenraed, A., Pobedinskas, P., Horemans, F., Diliën, H., Haenen, K., Cleij, T., Wagner, P., Thoelen, R., De Ceuninck, W., 2012. 'Development of multichannel quartz crystal microbalances for MIP-based biosensing. Phys. Status Solidi Appl. Mater. Sci 892–899.

Eersels, K., Lieberzeit, P., Wagner, P., 2016. 'A review on synthetic receptors for bioparticle detection created by surface-imprinting techniques-from principles to applications. ACS Sens. 1, 1171–1187.

Guo, X., Gao, S., Sang, S., Jian, A., Duan, Q., Ji, J., Zhang, W., 2016. Detection system based on magnetoelastic sensor for classical swine fever virus. Biosens. Bioelectron. 82, 127–131.

Hua, R.H., Huo, H., Li, Y.N., Xue, Y., Wang, X.L., Guo, L.P., Zhou, B., Song, Y., Bu, Z.G., 2014. 'Generation and efficacy evaluation of recombinant classical swine fever virus E2 glycoprotein expressed in stable transgenic mammalian cell line. PloS One 9, e106891.

Kupai, J., Razali, M., Buyuktiryaki, S., Kecili, R., Szekely, G., 2017. 'Long-term stability and reusability of molecularly imprinted polymers. Polym. Chem. 8, 666–673.

Lieberzeit, P.A., Chunta, S., Navakul, K., Sangma, C., Jungmann, C., 2016. 'Molecularly imprinted polymers for diagnostics: sensing high density lipoprotein and Dengue virus. In: Proceedings of the 30th Anniversary Eurosensors Conference - Eurosensors 2016, 168, pp. 101–104.

Lu, X., Shi, X., Wu, G., Wu, T., Qin, R., Wang, Y., 2017. 'Visual detection and differentiation of Classic Swine Fever Virus strains using nucleic acid sequence-based amplification (NASBA) and G-quadruplex DNAzyme assay. Sci. Rep. 7, 44211.

Moennig, V., 2000. 'Introduction to classical swine fever: virus, disease and control policy. Vet. Microbiol. 73, 93–102.

Moennig, V., Floegel-Niesmann, G., Greiser-Wilke, I., 2003. 'Clinical signs and epidemiology of classical swine fever: a review of new knowledge. Vet. J. 165, 11–20.

Mukherjee, P., Karam, A., Singh, U., Chakraborty, A.K., Huidrom, S., Sen, A., Sharma, I., 2018. 'Seroprevalence of selected viral pathogens in pigs reared in organized farms of Meghalaya from 2014 to 16. Vet. World 11, 42–47.

Mustafa, N.H., Allaudin, Z.N., Honari, P., Toung, O.P., Mohd-Lila, M.A., 2014. Detection of classical swine fever virus by a surface Plasmon resonance assay. Virol. Mycol. 3.

Naklua, W., Suedee, R., Lieberzeit, P.A., 2016. Dopaminergic receptor-ligand binding assays based on molecularly imprinted polymers on quartz crystal microbalance sensors. Biosens. Bioelectron. 81, 117–124.

OIE, World Organization for Animal Health, 2020. 'OIE-Listed Diseases, Infections and Infestations in Force in 2020.

Panyasing, Y., Thanawongnuwech, R., Ji, J., Gimenez-Lirola, L., Zimmerman, J., 2018. 'Detection of classical swine fever virus (CSFV) E2 and E(rns) antibody (IgG, IgA) in oral fluid specimens from inoculated (ALD strain) or vaccinated (LOM strain) pigs. Vet. Microbiol. 224, 70–77.

Petrini, S., Pierini, I., Giammarioli, M., Feliziani, F., De Mia, G.M., 2017. 'Detection of Classical swine fever virus infection by individual oral fluid of pigs following experimental inoculation. J. Vet. Diagn. Invest. 29, 254–257.

Phan, N.V.H., Sussitz, H.F., Ladenhauf, E., Pum, D., Lieberzeit, P.A., 2018. Combined layer/particle approaches in surface molecular imprinting of proteins: signal enhancement and competition. Sensors (Basel) 18.

Piletsky, S.S., Rabinowicz, S., Yang, Z., Zagar, C., Piletska, E.V., Guerreiro, A., Piletsky, S.A., 2017. 'Development of molecularly imprinted polymers specific for blood antigens for application in antibody-free blood typing. Chem Commun (Camb) 53, 1793–1796.

Poller, A.M., Spieker, E., Lieberzeit, P.A., Preininger, C., 2017. 'Surface imprints: advantageous application of Ready2use materials for bacterial quartz-crystal microbalance sensors. ACS Appl. Mater. Interfaces 9, 1129–1135.

Pomeranz, L.E., Reynolds, A.E., Hengartner, C.J., 2005. 'Molecular biology of pseudorabies virus: impact on neurovirology and veterinary medicine. Microbiol. Mol. Biol. Rev. 63, 462–500.

Postel, A., Austermann-Busch, S., Petrov, A., Moennig, V., Becher, P., 2018. 'Epidemiology, diagnosis and control of classical swine fever: Recent developments and future challenges. Transbound Emerg Dis 65 (Suppl 1), 248–261.

Postel, A., Oguzoglu, T.C., Schmeiser, S., Indenbirken, D., Alawi, M., Fischer, N., Grundhoff, A., Becher, P., 2015. 'Close relationship of ruminant pestiviruses and classical Swine Fever virus. Emerg. Infect. Dis. 21, 668–672.

Postel, A., Perez, L.J., Perera, C.L., Schmeiser, S., Meyer, D., Meindl-Boehmer, A., Rios, L., Austermann-Busch, S., Frias-Lepoureau, M.T., Becher, P., 2015. 'Development of a new LAMP assay for the detection of CSFV strains from Cuba: a proof-of-concept study. Arch. Virol. 160, 1435–1448.

Shi, Z., Sun, J., Guo, H., Tu, C., 2009. Genomic expression profiling of peripheral blood leukocytes of pigs infected with highly virulent classical swine fever virus strain Shimen. J. Gen. Virol. 90, 1670–1680.

Uribe-Campero, L., Monroy-García, A., Durán-Meza, A.L., Villagrana-Escareño, M.V., Ruíz-García, J., Hernández, J., Núñez-Palenius, H.G., Gómez-Lim, M.A., 2015. 'Plant-based porcine reproductive and respiratory syndrome virus VLPs induce an immune response in mice. Res. Vet. Sci. 102, 59–66.

Wang, R., Zhi, Y., Guo, J., Li, Q., Wang, L., Yang, J., Jin, Q., Wang, Y., Yang, Y., Xing, G., Qiao, S., Zhao, M., Deng, R., Zhang, G., 2015. Efficient purification of cell culture-derived classical swine fever virus by ultrafiltration and size-exclusion chromatography. Front. Agric. Sci. Eng. 2, 230–236.

Wangchareansak, T., Thitithanyanont, A., Chuakheaw, D., Gleeson, M.P., Lieberzeitc, P.A., Sangma, C., 2013. 'Influenza A virus molecularly imprinted polymers and their application in virus sub-type classification. J. Mater. Chem. B 1, 2190–2197.

Xu, J., Medina-Rangel, P.X., Haupt, K., Tse Sum Bui, B., 2017. 'Guide to the preparation of molecularly imprinted polymer nanoparticles for protein recognition by solid-phase synthesis. Methods Enzymol. 590, 115–141.